New Journal of Physics
The open-access journal for physics

Quasi-universal dipolar scattering in cold and ultracold gases

J L Bohn[1,4], M Cavagnero[2] and C Ticknor[3]

[1] JILA, NIST and Department of Physics, University of Colorado, Boulder, CO 80309-0440, USA
[2] Department of Physics and Astronomy, University of Kentucky, Lexington, KY 40506-0055, USA
[3] ARC Centre of Excellence for Quantum-Atom Optics and Centre for Atom Optics and Ultrafast Spectroscopy, Swinburne University of Technology, Hawthorn, VIC 3122, Australia
E-mail: bohn@murphy.colorado.edu, mike@pa.uky.edu and cticknor@swin.edu.au

New Journal of Physics **11** (2009) 055039 (18pp)
Received 9 January 2009
Published 14 May 2009
Online at http://www.njp.org/
doi:10.1088/1367-2630/11/5/055039

Abstract. We investigate the scattering cross section of aligned dipolar molecules in low-temperature gases. Over a wide range of collision energies relevant to contemporary experiments, the cross section declines in inverse proportion to the collision speed, and is given nearly exactly by a simple semiclassical formula. At yet lower energies, the cross section becomes independent of energy, and is reproduced within the Born approximation to within corrections due to the s-wave scattering length. While these behaviors are universal for all polar molecules, nevertheless interesting deviations from universality are expected to occur in the intermediate energy range.

[4] Author to whom any correspondence should be addressed.

Contents

1. Introduction

The energy dependence of scattering cross sections for atoms at ultralow collision energies is very simple. Either the cross section is nearly independent of energy, for distinguishable particles or identical bosons; or else the cross section vanishes altogether, for identical fermions. This behavior emerges in the limit where the deBroglie wavelength exceeds any natural length scale of the interatomic interaction, and the scattering is characterized by a single quantity, the s-wave scattering length a (alternatively, the p-wave scattering volume V_{p} for fermions). Although a dominates the threshold scattering, nevertheless its value must usually be determined painstakingly from experiments. This is because atomic interaction potentials, even those constrained by spectroscopic data on vibrational levels of the diatom, are usually insufficiently accurate to predict the scattering length [1].

By contrast, for low-energy collisions between polarized dipolar molecules, the near-threshold scattering is often approximately determined once the mass and dipole moment are known. The interaction between two molecules of reduced mass M and dipole moment μ is characterized by a dipole length, given by $D = M\mu^2/\hbar^2$.[5] Under a wide variety of circumstances, to be discussed in this paper, D is the dominant length scale and sets the threshold cross section, i.e. $\sigma \sim D^2$. Moreover, this circumstance holds for identical fermions as well as bosons. In this sense, the scattering of two dipoles is nearly universal at threshold, apart from possible modifications arising from s-wave scattering.

For realistic collisions in present-day experiments, however, collision energies are not always in this threshold region. When the threshold region is left behind, there is significant numerical evidence to suggest that a universal behavior still emerges, and that the cross section scales as $\sigma \sim D/K$, where K is the wave number of the relative motion [2]. The switch between the two types of behavior corresponds roughly to the natural energy scale of the dipolar interaction, $E_{\mathrm{D}} = \mu^2/D^3 = \hbar^6/M^3\mu^4$. Below this energy nonzero partial waves contribute only perturbatively, and only at large intermolecular separation; whereas at higher energies, many partial waves contribute and the scattering is semiclassical.

[5] D is determined, roughly, by equating a typical centrifugal energy, $\hbar^2/MD^2$, to a typical dipolar energy, μ^2/D^3. This is the same reasoning that leads to the definition of the Bohr radius, by equating centrifugal and Coulomb energies for hydrogen.

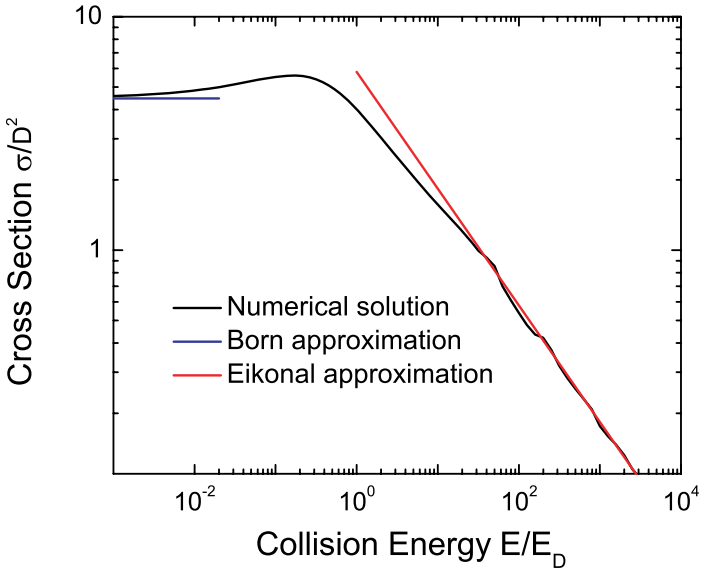

Figure 1. The total scattering cross section σ, averaged over all incident directions, for two distinguishable polarized dipoles. This cross section therefore includes contributions from both even and odd partial waves. In this calculation we have chosen boundary conditions that ensure the s-wave scattering length vanishes. In the low-energy limit, σ reduces to the Born approximation result (the sum of the two terms in equation (17), with $a = 0$, blue curve); while at high energies it is given by the semiclassical eikonal approximation in equation (33) (red curve). The solid line is a full numerical solution to the Schrödinger equation. Here $D = M\langle\mu_1\rangle\langle\mu_2\rangle/\hbar^2$ and $E_D = \hbar^6/M^3\langle\mu_1\rangle^2\langle\mu_2\rangle^2$ are the characteristic dipole length and energy scales defined in the text.

These two behaviors may thus be said to define the operational limit between 'cold' and 'ultracold' regimes of scattering for dipoles. We propose that the onset of cold collisions occurs when the temperature of the gas passes well below the molecule's rotational constant B_e (or else its Λ-doublet splitting) so that the orientational degrees of freedom freeze out. These temperatures are typically in the mK–K range. This cold collision regime, in which semiclassical scattering occurs, persists until the temperature gets as low as E_D (typically nK–μK temperatures for dipolar molecules). Temperatures below E_D define the ultracold regime, where true threshold scattering is apparent. Actual values of these temperatures depend strongly on the species considered and on the applied electric field.

Our goal in this paper is to make these ideas precise. We will illustrate the universal behavior of dipole–dipole scattering at low temperatures in the two regimes, and, more importantly, we will see the circumstances under which this universality fails. Figure 1 shows the basic elements of universality for dipole–dipole scattering. This figure plots the total scattering cross section σ, averaged over all incident directions, versus collision energy. Both quantities are presented in terms of the 'natural' units given above. The black curve is a complete numerical close-coupling calculation. At low energies, $E < E_D$, σ approaches a constant value that is well-approximated using the Born approximation (blue). For the sake of this comparison, we have carefully chosen the wave function's boundary conditions to achieve zero scattering

length. At higher energies $E > E_D$, σ falls off as $1/\sqrt{E}$, and is given by the semiclassical eikonal approximation (red). Both approximations will be derived below.

In this paper, we present alternative close-coupling calculations that reveal deviations from this universal behavior. For example, at threshold, the cross section can deviate substantially from the Born result. This occurs when threshold resonances in s-wave scattering dramatically increase the cross section above the Born result [3]–[6]. More interestingly, in the intermediate energy regime $E \approx E_D$ where neither approximation holds, our close-coupling calculations show that the behavior of the cross section versus energy depends on details of the physics on length scales small compared to D. For this reason, it is conceivable that elastic scattering experiments that probe deviations from universality will be an important tool in unraveling information on the short-range physics of close encounters. Finally, we also discuss the angle-dependence of cold collisions, in which the incident direction of the collision partners is varied with respect to the polarization axis; this is a measure of the importance of the anisotropy of the dipole–dipole interaction. These results should serve as simple and accurate guidelines to low-energy collision cross sections needed to understand scattering or thermal equilibration in contemporary experiments.

2. Formulation of the problem

For a pair of dipoles with reduced mass M and polarized in the $\hat{z}$-direction by an external field, the two-body Schrödinger equation reads (in CGS units)

$$\left[-\frac{\hbar^2}{2M}\nabla^2 + \langle\mu_1\rangle\langle\mu_2\rangle\frac{1-3\cos^2\theta}{R^3} + V_{SR}\right]\psi = E\psi. \tag{1}$$

Here the dipole interaction

$$V_d(\vec{R}) = \langle\mu_1\rangle\langle\mu_2\rangle\frac{1-3\cos^2\theta}{R^3}$$

is defined in terms of $\vec{R} = (R, \theta, \phi)$, the relative displacement of the two dipoles, and $\langle\mu_1\rangle$ and $\langle\mu_2\rangle$ are their induced dipole moments. These dipoles are field dependent, and their values are set by the field and the internal structure of the dipole. For the long range part of the physics where the dipole–dipole interaction dominates, this is an excellent approximation. Dipole orientations are relevant only when the dipole–dipole interaction μ^2/R^3 becomes comparable to the Stark energy $\mu\mathcal{E}$ that locks the dipole orientation to a laboratory axis. The radius at which this happens is typically far smaller than the dipole length D, hence this physics is subsumed into the short-range physics, which we do not treat explicitly. The validity of this approximation has already been suggested in [2], which did explicitly include the rotational substructure of the molecules, yet indicated universal behavior in the scattering. By ignoring internal molecular structure, we are in effect modeling molecules trapped in their absolute ground state, as in an optical dipole trap. In particular, we assume that inelastic scattering is disallowed, a topic taken up in the next paper of this issue [7].

The potential term V_{SR} represents all the short-range physics, i.e. the potential energy surface of chemical significance when the dipoles are close together. This detail will be specific to each pair of collision partners considered. To simplify the discussion, we will replace the complex details of V_{SR} by imposing a boundary condition at a fixed interparticle separation R_0. We will assert that the wave function ψ vanishes uniformly on this boundary. This is obviously

a simplification, but one that nevertheless allows comparison of alternative short-range physics. Alternative boundary conditions have been considered elsewhere, and ultimately will likely be necessary to exactly model experimental data [3, 4]. For our present purposes, however, we emphasize physics occurring on much larger length scales, at which the physics is accurately treated. Having made this approximation, we ignore $V_{\rm SR}$ in the following.

The resulting Schrödinger equation then admits a natural length scale $D = M\langle\mu_1\rangle\langle\mu_2\rangle/\hbar^2$ and a natural energy scale $E_{\rm D} = \hbar^6/M^3\langle\mu_1\rangle^2\langle\mu_2\rangle^2$. By recasting (1) in the scaled units $r = R/D$, $\epsilon = E/E_{\rm D}$, and by ignoring $V_{\rm SR}$, we arrive at the universal Schrödinger equation (assuming that the molecules have the same orientation relative to the field axis)

$$\left[-\frac{1}{2}\nabla^2 - \frac{2C_{20}}{r^3}\right]\psi = \epsilon\psi, \tag{2}$$

where $C_{20}(\theta, \phi) = (3\cos^2\theta - 1)/2$ is the standard reduced spherical harmonic [8]. Although the equation (2) has a universal form, nevertheless its *solutions* may depend on details of the short-range physics, represented here by the cutoff radius $r_0 = R_0/D$. Our main objective is to explore circumstances under which solutions are universal, i.e. independent of r_0, under the conditions of modern cold molecule experiments.

As a preliminary argument in this direction, let us consider the relative sizes of the two characteristic lengths D and R_0. For most atomic and molecular species, the size scale R_0 below which short-range physics can matter is of the order of the van der Waals length, which is typically $\sim$100 a_0, which is also the distance at which the internal fields generated by the dipoles are comparable to the applied field (at least for typical laboratory field strengths). By contrast, for molecules with typical 1 Debye dipole moments, D will be orders of magnitude larger. For example, in the OH radical, with $\mu = 1.68$ Debye, $D_{\rm OH} = 6770\ a_0$; for the representative alkali dimer KRb, with $\mu = 0.566$ Debye, $D_{\rm KRb} = 5740\ a_0$; and for the highly polar LiCs molecule with $\mu = 5.5$ Debye, we find $D_{\rm LiCs} = 6 \times 10^5\ a_0$. Correspondingly, the characteristic energies are low: $E_{\rm D,OH} = 445$ nK, while $E_{\rm D,KRb} = 83$ nK, and $E_{\rm D,LiCs} = 7$ pK. In making these estimates, we assume the molecules are completely polarized; D gets shorter, and $E_{\rm D}$ higher, if they are only partially polarized[6].

The finite size of R_0 can destroy universality in three ways. Firstly, at low energies, we will see that scattering cross sections are of order D^2. This would be spoiled by the geometric cross section $\propto R_0^2$, if R_0 were comparable to, or larger than, the dipole length D itself. However, we have just argued that this is usually not the case for polar molecules. Secondly, there is the possibility that the s-wave scattering length a is larger than D, and this would also alter the universal result at low energy. Indeed, this very idea has been invoked as a means of tuning the interaction between dipolar molecules [14]–[19][7] or else as a tool for probing details of these interactions [3]. Often, the effect of the scattering length is non-negligible, as we will see below.

The third instance where R_0 may matter is in the extreme high-energy limit, where the universal cross section falls as D/K, where K is the wave number. In this case the cross sections will again tend to the geometrical $\sim R_0^2$ for our artificially imposed hard wall, and will dominate at energies where $R_0^2 > D/K$, which translates to about 4.5 K in OH, well above Stark

[6] For species whose *magnetic* dipole moment mediates the interaction, these scales can be quite different. For atomic chromium, for instance, one finds $D_{\rm Cr} = 27\ a_0$, far smaller than its natural scattering length. A substantial body of literature now treats the complete details of the Cr–Cr interaction potential, for example [9, 10, 13].

[7] There are additional possibilities beyond the scattering length for tuning interactions, see [20].

decelerator energies, and at which point other degrees of freedom of the molecule are relevant. Thus non-universal behavior may not be a concern at 'high' energies either, from the standpoint of current experimental investigations.

In this paper we compute scattering cross sections for dipoles over a wide range of collision energies. We do this in three ways: (i) a fully numerical close-coupling expansion of the wave function in partial waves; (ii) a Born approximation that exhibits the correct universal behavior ($\sigma \sim D^2$) in the ultracold limit ($E < E_D$); and (iii) a semiclassical eikonal approximation that exhibits the correct universal behavior ($\sigma \sim D/K$) in the cold collision regime ($E > E_D$). We briefly describe these methods in the following subsections.

2.1. Close-coupling formalism

We expand the total wave function into partial waves in the conventional way:

$$\psi(r,\theta,\phi) = \frac{1}{r}\sum_{lm} F_{lm}(r)\,Y_{lm}(\theta,\phi), \tag{3}$$

where the radial functions F_{lm} satisfy a set of coupled-channel Schrödinger equations

$$-\frac{1}{2}\frac{\mathrm{d}^2 F_{lm}}{\mathrm{d}r^2} + \frac{l(l+1)}{2r^2}F_{lm} - \frac{2}{r^3}\sum_{l'} C^{(m)}_{ll'} F_{l'm} = \epsilon F_{lm}, \tag{4}$$

and the coupling matrix element is given by [8]

$$\begin{aligned} C^{(m)}_{ll'} &= \langle lm|C_{20}|l'm\rangle \\ &= (-1)^m\sqrt{(2l+1)(2l'+1)}\begin{pmatrix} l & 2 & l' \\ -m & 0 & m\end{pmatrix}\begin{pmatrix} l & 2 & l' \\ 0 & 0 & 0\end{pmatrix}. \end{aligned} \tag{5}$$

Owing to the cylindrical symmetry of the Hamiltonian, the angular momentum projection m is a good quantum number, and we can solve a separate set of coupled equations for each value of m. However, the boundary conditions of the wave function may not respect this symmetry, i.e. the incident wave could arrive from any direction, not just along the symmetry (z)-axis. Thus, we consider a complete sum over m in wave function (3). Similarly, symmetries of the $3-j$ symbols in (5) guarantee that each partial wave l is coupled only to the partial waves $l' = l, l \pm 2$ by the dipole interaction. Thus we can consider even partial waves separately from odd partial waves, and will do so in the following. For identical particles in the same internal state, these situations correspond to bosons and fermions, respectively.

Equation (4) admits as many linearly independent solutions as there are channels (lm). Individually, they are defined by the boundary conditions (for each m)

$$\begin{aligned} F^{l'm}_{lm}(r = r_0) &= 0, \\ F^{l'm}_{lm}(r \to \infty) &= \delta_{ll'}\mathrm{e}^{-\mathrm{i}(kr - l'\pi/2)} - S^{(m)}_{ll'}\mathrm{e}^{\mathrm{i}(kr-l'\pi/2)}, \end{aligned} \tag{6}$$

where $k = \sqrt{2\epsilon} = DK$ is the wave number in dipole units. These scattering boundary conditions serve to define the scattering matrix $S^{(m)}_{ll'}$. From this matrix one can construct the scattering amplitude describing scattering in direction $\hat{k}_\mathrm{f} = (\theta,\phi)$ from an incident direction $\hat{k}_\mathrm{i}$ [22, 23]:

$$f(\hat{k}_\mathrm{i},\hat{k}_\mathrm{f}) = -\frac{2\pi}{k}\sum_{ll'm} \mathrm{i}^l Y^*_{lm}\left(\hat{k}_\mathrm{i}\right) T^{(m)}_{ll'} \mathrm{i}^{-l'} Y_{l'm}\left(\hat{k}_\mathrm{f}\right), \tag{7}$$

in terms of the T matrix, $T = \mathrm{i}(S - I)$. By integrating over the final directions, we arrive at the total cross section for dipoles incident along $\hat{k}_\mathrm{i}$:

$$\frac{\sigma_\mathrm{tot}(\hat{k}_\mathrm{i})}{D^2} = \int \mathrm{d}\phi \mathrm{d}(\cos\theta)|f|^2 = \frac{4\pi}{k}\Im f\left(\hat{k}_\mathrm{i}, \hat{k}_\mathrm{i}\right). \tag{8}$$

This last line is the familiar optical theorem result. This is the type of cross section that can be measured in cold beam experiments, where, say, one species is trapped and the other is incident on the trap from the terminus of a Stark decelerator. If the molecules are magnetically trapped, then an electric field can be applied at an arbitrary angle relative to the collision axis [24].

Finally, the total cross section, averaged over an assumed isotropic distribution of initial directions, is

$$\frac{\sigma}{D^2} = \int \mathrm{d}\hat{k}_\mathrm{i} \frac{\sigma_\mathrm{tot}\left(\hat{k}_\mathrm{i}\right)}{D^2} = \frac{\pi}{k^2}\sum_{ll'm}\left|T_{ll'}^{(m)}\right|^2. \tag{9}$$

This cross section is more relevant to *in situ* collisions in a trap, which serve to re-thermalize the gas and provide evaporative cooling.

Numerical solutions to coupled-channel equations (4) are determined using a variable stepsize version of Johnson's algorithm [26]. To ensure convergence of total cross sections, we include partial waves up to $l \sim 100$ at the highest collision energies of $\epsilon = 10^4$. Vice versa, at the lowest collision energies we can get away with partial waves up to $l \sim 30$, but must apply boundary conditions (6) as far out as $r = 20\,000$.

2.2. Born approximation

At the lowest collision energies, the Wigner threshold laws are well known to be different for dipolar interactions than for, say, van der Waals interactions. The elastic scattering phase shift δ_l in partial wave $l > 0$, due to a potential with $1/r^s$ long-range behavior, is [25]

$$\tan\delta_l \sim Ak^{2l+1} + Bk^{s-2}, \tag{10}$$

for some constants A and B that depend on short-range details. The first term in (10) arises from the action of the short-range potential, while the second is due to purely long-range scattering *outside* the centrifugal barrier. For the van der Waals potential ($s = 6$), both contributions go to zero faster than $\sim k$ at zero energy, and do not contribute to the threshold cross section. However, for the dipole–dipole interaction ($s = 3$), the second term is $\sim k$ for all partial waves. The contribution to the cross section, $\propto \sin^2\delta_l/k^2$, is then independent of energy in all partial waves, and this cross section arises from long-range scattering [11, 12].

This circumstance leads to the applicability of the Born approximation in threshold scattering of dipoles [15], [17]–[19], [27, 28]. At ever lower collision energy, scattering occurs at ever larger values of r outside the barrier. But at long range the dipole–dipole interaction $\propto 1/r^3$ is weak, and the perturbative Born approximation is applicable. These remarks do not apply, however, to s-wave scattering, where there is no barrier.

The Born approximation for the scattering amplitude reads

$$f(\hat{k}_\mathrm{i},\hat{k}_\mathrm{f}) = -\frac{1}{2\pi}\int \mathrm{d}^3 r\, \mathrm{e}^{-\mathrm{i}\vec{k}_\mathrm{f}\cdot\vec{r}}\, V_\mathrm{d}(\vec{r})\mathrm{e}^{\mathrm{i}\vec{k}_\mathrm{i}\cdot\vec{r}}. \tag{11}$$

Replacing each plane wave by its standard partial wave expansion and re-arranging yields

$$\begin{aligned} f(\hat{k}_\mathrm{i},\hat{k}_\mathrm{f}) = & -\frac{1}{2\pi}\int \mathrm{d}^3 r \left(-\frac{2}{r^3}\right) C_{20}(\hat{r})\, 4\pi \sum_{l'm'} \mathrm{i}^{-l'} Y_{l'm'}(\hat{k}_\mathrm{f}) Y^*_{l'm'}(\hat{r})\, j_{l'}(kr) \\ & \times 4\pi \sum_{lm} \mathrm{i}^{l} Y^*_{lm}(\hat{k}_\mathrm{i}) Y_{lm}(\hat{r})\, j_l(kr). \end{aligned} \tag{12}$$

Consolidating the integrals into radial and angular varieties, we arrive at

$$f(\hat{k}_\mathrm{i},\hat{k}_\mathrm{f}) = 2\pi \sum_{ll'm} \mathrm{i}^{l} Y^*_{lm}(\hat{k}_\mathrm{i}) C^{(m)}_{ll'} \Gamma_{ll'} \mathrm{i}^{-l'} Y_{l'm'}(\hat{k}_\mathrm{f}), \tag{13}$$

where $C^{(m)}_{ll'}$ is the angular integral (5) defined above, and $\Gamma_{ll'}$ is the radial integral

$$\begin{aligned} \Gamma_{ll'} &= 8\int_0^\infty r^2\, \mathrm{d}r \frac{j_l(kr)\, j_{l'}(kr)}{r^3} \\ &= \frac{\pi\,\Gamma((l+l')/2)}{\Gamma((-l+l'+3)/2)\Gamma((l+l'+4)/2)\Gamma((l-l'+3)/2)}. \\ &= \begin{cases} \dfrac{32}{l(l+1)}, & l' = l, \\ \dfrac{32}{3(l+1)(l+2)}, & l' = l+2. \end{cases} \end{aligned} \tag{14}$$

Comparing Born result (13) with expression (7) identifies the T-matrix in the Born approximation as

$$T^{(m),\mathrm{Born}}_{ll'} = -kC^{(m)}_{ll'}\Gamma_{ll'}. \tag{15}$$

The Born approximation must be applied with a caveat. For purely s-wave scattering, where $l = l' = 0$, the matrix element $C^{(0)}_{00}$ vanishes, and so therefore does the T-matrix element $T^{(0),\mathrm{Born}}_{00}$. The Born approximation is therefore mute on the question of s-wave scattering. As argued above, s-wave scattering, described by a scattering length a, is part of the non-universal behavior of scattering anyway. To produce realistic scattering results, it is possible to supplement T^{Born} with an empirical s-wave contribution, which is determined from the full close-coupling calculations [14], [17]–[19], [21].

Summarizing all these results, the threshold cross section in the Born approximation, averaged over incident directions, is given by the incoherent sum

$$\frac{\sigma_\mathrm{Born}}{D^2} = \frac{\pi}{k^2}\sum_{ll'm}\left|T^{(m),\mathrm{Born}}_{ll'}\right|^2. \tag{16}$$

Evaluating the sums, the even and odd partial wave cross sections at threshold can be given as

$$\begin{aligned} \sigma^\mathrm{e}_\mathrm{thresh} &= \sigma^\mathrm{e}_\mathrm{Born} + 4\pi a^2 = 1.117D^2 + 4\pi a^2, \\ \sigma^\mathrm{o}_\mathrm{thresh} &= \sigma^\mathrm{o}_\mathrm{Born} = 3.351D^2, \end{aligned} \tag{17}$$

where $4\pi a^2$ allows for the existence of a scattering length a, which is not determined in the Born approximation. For identical particles, cross sections (17) must be multiplied by 2, as usual; for distinguishable particles, both even and odd partial waves are possible, and these cross sections are to be added.

Low-energy limits (17) were independently verified in near-threshold calculations using a coupled-channel adiabatic representation [5, 6], which also illustrated how threshold angular distributions are affected by the competition between long-range (Born) coupling and s-wave scattering resonances, as discussed in section 4.

2.3. Eikonal approximation

At sufficiently high energies, a semi-classical analysis yields the simple D/K scaling of the cross section. Note, in reference to figure 1, that the deBroglie wavelength becomes smaller than the natural dipole length scale, $2\pi/K < D$, when $E > 2\pi^2 E_{\rm D}$. This marks the onset of semi-classical scattering. This semi-classical onset can lie at μK temperatures, or even colder, owing to the large dipole length scale and therefore the small value of $E_{\rm D}$. Many partial waves contribute to the scattering amplitude in the semi-classical regime, and differential cross-sections are increasingly concentrated in the forward direction.

The eikonal method was long ago developed to find approximate scattering solutions of wave equations such as (2) valid in the semi-classical or ray-optics limit, in which the potential is assumed to vary little on the scale of the wavelength. A derivation of the eikonal wavefunction will not be given here, as it can be found in familiar texts [29] and in a comprehensive review paper by Glauber [30], and in the nuclear physics literature [31]. Suffice it to say that a phase-amplitude *ansatz*, coupled with the assumption of a slowly varying amplitude, leads directly to an approximate wavefunction

$$\psi(\vec{r}) = \mathrm{e}^{\mathrm{i}\vec{k}_i\cdot\vec{r}} \exp\left[-\frac{\mathrm{i}}{k}\int^z V(b,\phi,z')\,\mathrm{d}z'\right]. \tag{18}$$

Following Glauber, this wavefunction is expressed in cylindrical coordinates with a new quantization (or z)-axis aligned with the average collision momentum, $\vec{k}_{\rm avg} = (\vec{k}_{\rm i} + \vec{k}_{\rm f})/2$. The cylindrical radius about this axis, b, can be associated with a classical impact parameter: ϕ is the azimuthal angle about the quantization axis. Due to the shift of quantization axis away from the direction of the applied field, $\vec{\mathcal{E}}$, we now note the field direction explicitly in the potential $V(\vec{r}) = [1 - 3(\hat{r}\cdot\hat{\mathcal{E}})^2]/r^3$.

The two factors in the eikonal wavefunction are familiar in the context of the one-dimensional Wentzel–Kramers–Brillouin (WKB) method, where they coincide with an expansion of the WKB phase $\mathrm{i}\int \mathrm{d}z\sqrt{2(\epsilon - V)} \approx \mathrm{i}kz - (\mathrm{i}/k)\int \mathrm{d}z V$ to first order in V/ϵ. Accordingly, we anticipate that the eikonal method will be most accurate when the incident energy is large compared to the magnitude of the dipole–dipole interaction, a more stringent criterion than the semi-classical constraint noted above.

The analysis of scattering amplitudes associated with the approximate eikonal wavefunction is simplified by a judicious choice of coordinates. Note, in particular, that the momentum transfer $\vec{q} = \vec{k}_{\rm i} - \vec{k}_{\rm f}$ is orthogonal to the quantization axis defined by $\vec{k}_{\rm avg}$. For simplicity, we define an x-axis along $\vec{q}$, in which case the y-axis is orthogonal to the collision plane and lies along $\vec{k}_{\rm avg} \times \vec{q}$. In this reference frame, the impact parameter is written in

vector form as $\vec{b} = b\cos(\phi)\hat{x} + b\sin(\phi)\hat{y}$, and the relative displacement of the dipoles is $\vec{r} = \vec{b} + z\hat{k}_{\rm avg}$.

Insertion of the eikonal wavefunction, valid where the potential is non-negligible, into the integral equation for scattering leads to the eikonal scattering amplitude

$$f^{\rm Ei}(\vec{k}_{\rm f}, \vec{k}_{\rm i}) = \frac{k}{2\pi {\rm i}} \int b\, {\rm d}b\, {\rm d}\phi {\rm e}^{{\rm i}qb\cos(\phi)} \left[{\rm e}^{{\rm i}\chi(\vec{b})} - 1\right], \tag{19}$$

where $k = |k_{\rm i}| = |k_{\rm f}| = \sqrt{2\epsilon}$, $q = |\vec{q}| = 2k\ \sin(\theta_s/2)$, and where the eikonal phase is

$$\chi(\vec{b}) = -\frac{1}{k}\int_{-\infty}^{\infty} {\rm d}z'\, V(b, \phi, z'). \tag{20}$$

With the explicit form of the dipole–dipole potential

$$V(b, \phi, z) = \frac{1}{(b^2+z^2)^{3/2}}\left[1 - 3\frac{(\vec{b}\cdot\hat{\mathcal{E}} + z\hat{k}_{\rm avg}\cdot\hat{\mathcal{E}})^2}{b^2+z^2}\right], \tag{21}$$

the phase is readily evaluated; setting $\sigma = z/b$ one finds

$$\chi = -\frac{1}{kb^2}\left[\int_{-\infty}^{\infty}\frac{{\rm d}\sigma}{(1+\sigma^2)^{3/2}} - 3(\hat{b}\cdot\hat{\mathcal{E}})^2\int_{-\infty}^{\infty}\frac{{\rm d}\sigma}{(1+\sigma^2)^{5/2}} - 3(\hat{k}_{\rm avg}\cdot\hat{\mathcal{E}})^2\int_{-\infty}^{\infty}\frac{\sigma^2{\rm d}\sigma}{(1+\sigma^2)^{5/2}}\right]. \tag{22}$$

The integrals are straightforward, giving

$$\chi = -\frac{2}{kb^2}\left[1 - (\hat{k}_{\rm avg}\cdot\hat{\mathcal{E}})^2 - 2(\hat{b}\cdot\hat{\mathcal{E}})^2\right]. \tag{23}$$

Referring the electric field to our coordinate axes ($\hat{x} = \hat{q}$, $\hat{y} = \hat{k}_{\rm avg}\times\hat{q}$, $\hat{k}_{\rm avg}$)

$$\hat{\mathcal{E}} = \sin\,\alpha\,\cos\,\beta\hat{x} + \sin\alpha\,\sin\beta\hat{y} + \cos\alpha\hat{k}_{\rm avg}, \tag{24}$$

the phase is simply

$$\chi(b, \phi) = \frac{2}{kb^2}\sin^2\,\alpha\,\cos(2\phi - 2\beta). \tag{25}$$

The eikonal amplitude now has the form

$$f^{\rm Ei} = \frac{k}{2\pi{\rm i}}\int b\,{\rm d}b\,{\rm d}\phi\,{\rm e}^{{\rm i}qb\cos\phi}\left[\exp\left\{{\rm i}\frac{2}{kb^2}\sin^2\,\alpha\,\cos(2\phi - 2\beta)\right\} - 1\right]. \tag{26}$$

Explicit evaluation of the resulting integrals has proven quite difficult. However, to extract total cross-sections, Glauber's general proof of unitarity of the eikonal approximation [30] permits use of optical theorem (8).

For forward scattering, $q = 0$ and the first phase vanishes identically. Expressing the result in terms of the orbital angular momentum $l = kb$ gives

$$f^{\rm Ei}(\hat{k}_{\rm i}, \hat{k}_{\rm i}) = \frac{1}{2\pi{\rm i}k}\int \ell\,{\rm d}\ell\,{\rm d}\phi\left[\exp\left\{{\rm i}\frac{2k}{\ell^2}\sin^2\alpha\cos(2\phi - 2\beta)\right\} - 1\right], \tag{27}$$

but note that this appears undetermined since $\hat{q}$ and, consequently, $\hat{x}$ and $\hat{y}$ are not defined when $q = 0$! In this limit, $\alpha = \arccos(\hat{k}\cdot\hat{\mathcal{E}})$ is well-defined, but $\beta = \arctan(\hat{y}\cdot\hat{\mathcal{E}}/\hat{x}\cdot\hat{\mathcal{E}})$ is not. Fortunately, it is easy to show that the azimuthal integral is independent of β, with the result

$$f^{\rm Ei}(\hat{k}_{\rm i}, \hat{k}_{\rm i}) = \frac{1}{{\rm i}k}\int \ell\,{\rm d}\ell\left[J_0\left(\frac{2k}{\ell^2}\sin^2\alpha\right) - 1\right]. \tag{28}$$

From the optical theorem, the total cross section is then

$$\frac{\sigma^{\rm Ei}}{D^2} = \frac{4\pi}{k^2}\int_0^\infty \ell\,{\rm d}\ell\left[1 - J_0\left(\frac{2k}{\ell^2}\sin^2\alpha\right)\right]. \tag{29}$$

This result provides some insight into partial wave analysis in the semi-classical regime, which approximately separates into two regions: for $l < \sqrt{k}\sin(\alpha)$, the integrand is nearly linear in l, while for larger l it declines steeply as $k^2\sin^4(\alpha)/l^3$. Using these approximations, the integral evaluates to $k\sin^2(\alpha)$, the exact result (32) given below.

More carefully, we set

$$s = \frac{2k}{\ell^2}\sin^2\alpha, \qquad \ell{\rm d}\ell = -k\sin^2\alpha\frac{{\rm d}s}{s^2}, \tag{30}$$

and so express the total eikonal cross section in terms of a dimensionless integral

$$\frac{\sigma^{\rm Ei}}{D^2} = \frac{4\pi\sin^2\alpha}{k}\int_0^\infty \frac{{\rm d}s}{s^2}\left[1 - J_0(s)\right]. \tag{31}$$

The integral evaluates to unity, with the result

$$\frac{\sigma^{\rm Ei}_{\rm tot}(\hat{k}_{\rm i})}{D^2} = \frac{4\pi}{k}\left[1 - \left(\hat{k}_{\rm i}\cdot\hat{\mathcal{E}}\right)^2\right]. \tag{32}$$

Remarkably, the cross section is identically zero when the direction of incidence is aligned with the field axis. Since, as will be discussed below, this semi-classical cross section accurately describes dipolar collisions in the temperature range currently accessible experimentally, there are a variety of observables which might test this angle-dependence of the total elastic cross section. While equilibrium properties of the gas would not be sensitive to the angle-dependence, non-equilibrium properties, such as transmission of fast dipoles through a trapped dipolar gas, would be expected to show strong dependence on the alignment of the beam with the field axis.

Averaged over incident directions within a confined gas, one then expects

$$\frac{\sigma_{\rm Ei}}{D^2} = \frac{8\pi}{3k} = \frac{8\pi}{3KD}, \tag{33}$$

which is the final result. As shown in figure 1, Glauber's method yields not only the correct scaling, but quantitatively reproduces the universal results discovered in close-coupling calculations [2].

The basic structure of this result was surmized by Gallagher [32] in a study of Rydberg–Rydberg collisions: from the uncertainty principle, an interaction of energy $1/b^3$ and lasting for a duration b/k, should satisfy $1/b^2k \sim 1$ in scaled units, so that $\sigma \sim b^2 = 1/k$. Using an isotropic $-1/r^3$ interaction, DeMille *et al* [33] also applied the eikonal approximation and determined a cross section $\sigma/D^2 = 2\pi^2/k$. Kajita's Fourier technique [34] yields the high-velocity result $\sigma/D^2 = 40\pi\sqrt{2}/3k$. In essence, this technique is a renormalized perturbation theory that can produce a unitarity-limited upper bound to the cross section. Thus while it obtains the correct $1/k$ scaling, it overestimates the correct eikonal result.

3. The rise and fall of universal scattering

Figure 1 has already presented the message of universality, in that the Born and eikonal limits are achieved in the appropriate energy ranges. However, the calculations in this figure were

carefully selected to have zero scattering length, by choosing an appropriate cutoff radius r_0. By changing r_0, we are able to generate any scattering length a. Experimentally, the value of a can be altered by changing the electric or magnetic field strength. Changing r_0 could also change the scattering phase shift of any other partial wave. However, this is only likely for those partial waves whose centrifugal barrier lie below the collision energy, because these partial waves are the only ones to probe physics at the scale of r_0.

The importance of the centrifugal barriers in determining the range of applicability of the low-energy (Born) scaling was emphasized in [5, 6], through adiabatic calculations which converge much more rapidly than close-coupling calculations at the lowest energies. The adiabatic curves have pronounced barriers (in all but the s-wave channel) separating repulsive centrifugal behavior at large r from attractive dipolar behavior at small r. The heights of the lowest barriers (approximately coincident with E_D) determine the range of energy over which the threshold behavior of the cross section is approximately constant. They also suggest the sensitivity to r_0 at intermediate energies, where incident flux can surmount the barrier.

Figure 2 shows the effect of changing r_0 on the 'universal' cross section from figure 1. In figure 2(a) is shown the result for even partial waves. The black line is the $a = 0$ result, and it amicably reaches the universal Born and eikonal limits. The other curves employ values of r_0 that produce scattering lengths of $a = 0.1D$ (red) and $a = -0.1D$ (blue). This change has made a significant difference in the low-energy limit, where now the Born approximation is merely a lower limit to the cross section. Note also that for $a < 0$ the cross section initially decreases with increasing energy, just as it does for alkali atoms [35]

However, at higher energies $E > E_D$, this change in r_0 has no effect on σ. One way to look at this is that the phase shifts have changed for many partial waves, but because there are so many of them added together to get the cross section, these changes average out. Another point of view is that the semiclassical scattering occurs at high impact parameter, and is thus indifferent to what happens at $r = r_0$. In the intermediate energy range, the change is still quite significant, since phase shifts are changing for only those few partial waves that skip over their centrifugal barriers.

Figure 2(b) shows the same circumstance, but for odd partial waves. The same three values of r_0 are employed here, and so the three curves are labeled by the scattering lengths from part (a). In this case the cross sections always approach the Born limit, since there is no aberrant s-wave scattering to derail them. In the high-energy limit, too, σ is again insensitive to r_0. It is only in the intermediate energy range that a small deviation is seen. This suggests that for odd partial waves the behavior of the cross section is indeed nearly universal. This would be true, for example, in collisions of fermionic molecules (e.g. $^{40}K^{87}Rb$ [36]) in identical hyperfine states.

To further emphasize the consequence of an s-wave scattering length, figure 3 reports the cross section σ for the even partial waves as a function of r_0, in the threshold limit, using $E/E_D = 10^{-3}$. The range of r_0 shown here corresponds to a complete cycle of the scattering length from zero, through infinity, and back to zero again. Consequently, the numerically evaluated cross section shows a resonance, at which point the cross section is determined by a^2, not D^2. Even away from the resonance peak, the s-wave contribution can significantly increase the cross section. We are thus led to conclude that universality at low energies, in cases where s-wave scattering is allowed, is similar to the universality for atoms. Namely, the form of the cross section (independent of energy) is universal, but its value relies on a (field-dependent)

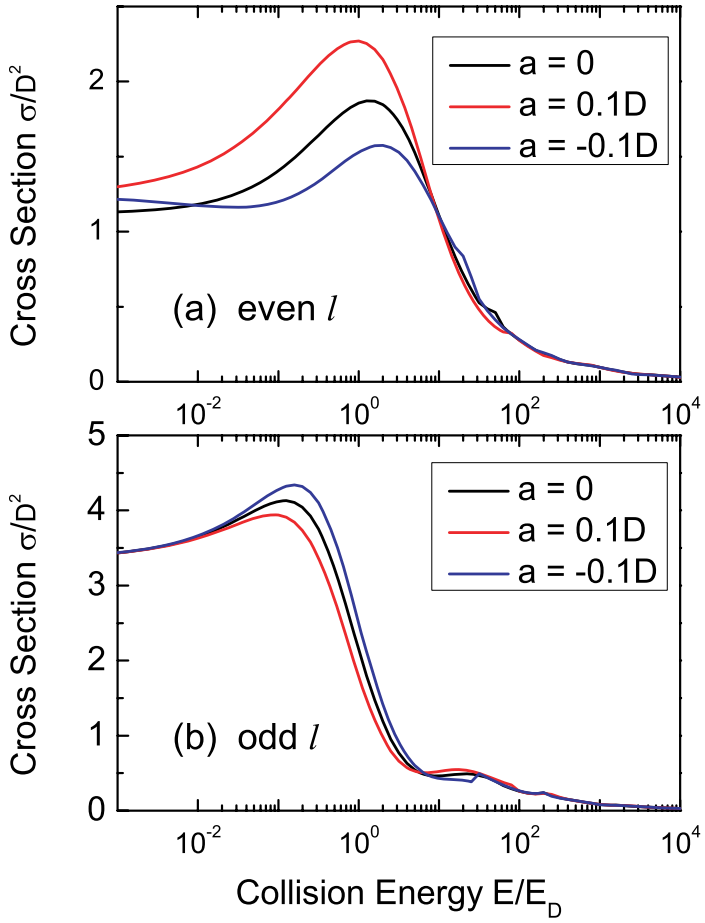

Figure 2. Cross sections as in figure 1, but separated into contributions from all even (a) or all odd (b) partial waves. In contrast to figure 1, here the cross section is plotted on a linear scale, to emphasize differences between different curves. In each case, three different values of the cutoff radius r_0 are chosen, corresponding to three different s-wave scattering lengths a, as indicated in the legend. The same three values of r_0 are used in both panels. In each panel differences in the three curves demonstrate the breakdown of universality. Elastic scattering is thus much more universal for odd partial waves (identical fermions) than for even partial waves (identical bosons or distinguishable particles).

scattering length that must be determined empirically. The Born approximation does provide a useful lower limit, however. For odd partial waves, while resonances exist, they are shape resonances, hence narrow at low energies and less likely to destroy universal behavior.

The s-wave contribution to the Hamiltonian nominally vanishes, since $C_{00}^{(0)} = 0$. However, it is not unreasonable that s-wave scattering has a strong influence near threshold. To see this, we evaluate an effective s-wave interaction at long range, via its coupling to the $l = 2$ partial wave, in second-order perturbation theory (compare [37]):

$$V_0(r) \approx -\frac{|2C_{02}^{(0)}/r^3|^2}{l(l+1)/2r^2} = -\frac{C_4}{r^4}, \tag{34}$$

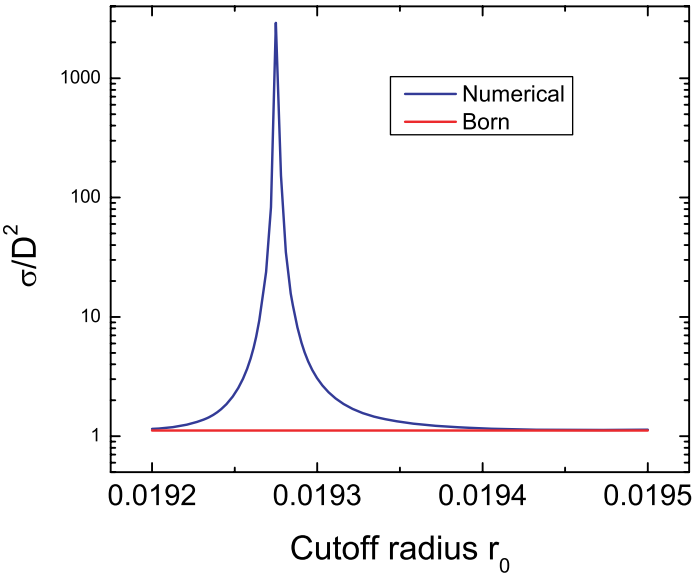

Figure 3. Cross section σ for various values of the cutoff radius r_0. The numerically determined cross section is always larger than the Born approximation, sometimes significantly higher, due to a large s-wave scattering length.

where, in dipole units and using $l = 2$, the coefficient is $C_4 = \frac{4}{3}\sqrt{5}$. This in turn leads to a characteristic length scale for the s-wave interaction, analogous to the characteristic van der Waals length,

$$r_4 = \left(\frac{2\mu C_4}{\hbar^2}\right)^{1/2} = (2C_4)^{1/2}. \tag{35}$$

In dipole units, this is $r_4 = 1.09D$, comparable to the dipole length itself. Based on this consideration, it is perhaps not too surprising that s-wave scattering plays a significant role.

4. Dependence on incident angle

Thus far we have focused on the cross section as averaged over all incident angles. One of the interesting aspects of the dipole–dipole interaction, however, is its anisotropy. The cross section $\sigma_{\rm tot}(\theta_{\rm i})$ may therefore depend on the angle $\theta_{\rm i} = \arccos(\hat{k}_{\rm i} \cdot \hat{\mathcal{E}})$ of the incident collision axis, with respect to the polarization direction. This cross section is easily calculated numerically from (8), and also from the useful eikonal estimate (32).

To show the utility of the eikonal expression, we present in figure 4 $\sigma_{\rm tot}$ versus $\theta_{\rm i}$, for a collision energy $E/E_{\rm D} = 10^4$ where the eikonal approximation should be fairly accurate. The total close-coupled cross section (black solid line) is the sum of contributions from even and odd partial waves. Note that the contributions from these two sets of partial waves are nearly equal here in the semiclassical limit where many partial waves contribute, and effects of dipole-indistinguishability are small. The angular distribution of each shows oscillations, but in the sum, representing distinguishable particles, the angular dependence is smooth. Moreover, for

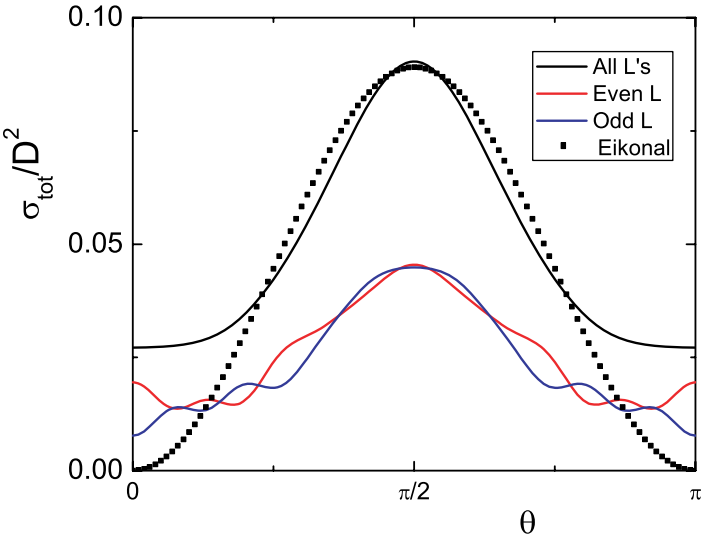

Figure 4. Dependence of scattering cross sections $\sigma_{\rm tot}$ on the incident angle $\theta_{\rm i}$ between the collision axis and the polarization axis of the dipoles. This calculation is performed at a high collision energy, $E/E_{\rm D} = 10^4$. The distribution is well-approximated using the eikonal result (32), except when the collision and polarization axes nearly coincide.

angles where the collision axis is orthogonal to the polarization axis, $\theta_{\rm i} \approx \pi/2$, the eikonal approximation (dotted line) is quite good.

A major deviation occurs, however, for dipoles aligned parallel to the collision axis. Here the eikonal result calls for vanishing cross section, whereas the close coupling calculation yields a nonzero cross section. For $\theta_{\rm i} = 0$, the incident wave $e^{i\vec{k}_{\rm i}\cdot\vec{r}}$ is invariant under rotations about the field axis, and so contains only $m = 0$ partial waves. It is not too surprising that a semi-classical analysis will break down for low-m states. Furthermore, for $m = 0$ states, the wavefunction is large where the potential is strongest (near $r = 0$), so the eikonal assumption $V/\epsilon \ll 1$ is no longer valid. Most interesting about this deviation from eikonal behavior, is the importance of back-scattering from the strong potential in this geometry, as indicated by the pronounced difference between even and odd partial waves. Observations near $\theta_{\rm i} = 0$ will accordingly be most sensitive to exchange scattering, and, presumably, to short-range physics.

Cross-section variations with the angle of incidence have also been studied at low energies [5, 6]. When the s-wave scattering length is negligible, a universal anisotropic distribution is obtained, entirely due to long-range scattering. However, when the s-wave scattering length dominates, near the peak in figure 3, a completely isotropic distribution is found, as in the case of ultracold atomic collisions. Interestingly, this implies that effects of anisotropy are to be seen at the lowest temperatures only when the scattering length is small, and cross sections are accurately represented by the Born approximation.

5. What this means for you

Scaled units are fine for proving a theoretical point, as we have hoped to do here. However, since dipole length scales vary widely between different molecules and at different electric field strengths, it is also useful to consider specific examples that measure cross sections in $\rm cm^2$.

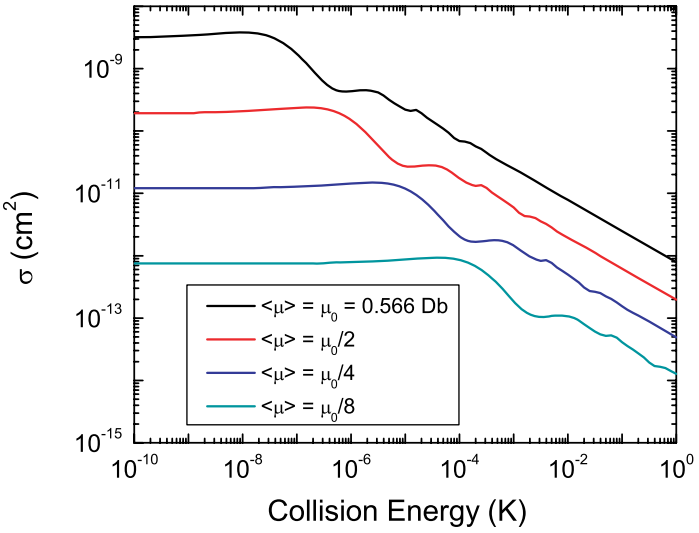

Figure 5. Elastic cross section for scattering of pairs of fermionic $^{40}K^{87}Rb$ molecules in identical internal states, averaged over incident directions. This calculation is based on the 'universal' calculation that includes only dipole–dipole interactions. The top curve is the cross section for fully polarized molecules with dipole moment $\langle\mu\rangle = 0.566$ Debye. The dipole is halved for each successively lower curve.

Before presenting such an example, we first recapitulate our main results, cast in terms of the explicit dimensionful factors. Scattering in the ultracold limit is given by

$$\begin{aligned}\sigma^{\mathrm{e}}_{\mathrm{thresh}} &= \sigma^{\mathrm{e}}_{\mathrm{Born}} + 4\pi a^2 = 1.117\frac{M^2\langle\mu_1\rangle^2\langle\mu_2\rangle^2}{\hbar^4} + 4\pi a^2,\\ \sigma^{\mathrm{o}}_{\mathrm{thresh}} &= \sigma^{\mathrm{o}}_{\mathrm{Born}} = 3.351\frac{M^2\langle\mu_1\rangle^2\langle\mu_2\rangle^2}{\hbar^4}.\end{aligned} \tag{36}$$

The semiclassical result, valid for cold collisions, $E > E_{\mathrm{D}} = \hbar^6/M^3\langle\mu_1\rangle^2\langle\mu_2\rangle^2$, is

$$\sigma_{\mathrm{Ei}} = \frac{8\pi}{3}\frac{\langle\mu_1\rangle\langle\mu_2\rangle}{\hbar}\sqrt{\frac{M}{2E}}. \tag{37}$$

(Recall that our eikonal derivation does not distinguish between even and odd partial wave contributions. To a good approximation, both the even and odd contributions would be half this value.) These formulae show explicitly that the cross sections at low and high energy differ not only in their dependence on energy, but also in their dependence on the parameters—reduced mass and dipole moments—of the molecules.

To give a concrete example, consider the ground-state $^{40}K^{87}Rb$ molecules that were recently produced at temperatures of several hundred nK [36]. This molecule has a dipole moment of 0.566 Debye, and, being a fermion, would collide only in odd partial waves if it is trapped in a single quantum state. We therefore plot in figure 5 the odd partial wave cross section computed above, but cast in realistic units for this molecule. The largest cross section corresponds to the full dipole moment, $\langle\mu\rangle = 0.566$ Debye. Each successively lower curve divides the dipole moment into half from the previous one. For this reason, each low-energy cross section drops by a factor of 16 from the one above, while at high energy each cross

section drops by a factor of 4. Because the dipole moment is something that can be changed by the application of a greater or lesser electric field, cross sections spanning this stunning range of magnitudes should be observable in experiments.

Also interesting is the energy scale encompassed by this figure. In the experiment, the gas is trapped at a temperature of 350 nK. At low electric field values, hence low dipole moments, these molecules are in the ultracold regime, and scatter according to the Born prescription. At higher fields, however, E_D approaches the temperature of the gas, and experiments might start to observe the non-universal behavior of the scattering.

In summary, we have characterized the total scattering cross section for dipolar molecules, both in the cold limit $E_D < E < B_e$, and in the ultracold limit $E < E_D$. The behavior of this scattering is universal for cold collisions, and nearly so for ultracold collisions. In the temperature regime intermediate between these two, universality breaks down, and empirical cross sections will likely reveal information about the intermolecular potential energy surface. We expect these conclusions to hold in the regime where the molecules are sufficiently polarized that the dipole length D exceeds any other natural scale of the interaction. Moreover, the dipoles should remain well polarized in the lab even down to small intermolecular separation, i.e. $\mu\mathcal{E} \gg \mu^2/R^3$ for $r \geqslant 100\, a_0$.

Acknowledgments

We acknowledge the financial support from the NSF (J L B), the ARC (C T), and the University of Kentucky (M C), and also discussions with D DeMille.

References

[1] Weiner J, Bagnato V S, Zilio S and Julienne P S 1999 *Rev. Mod. Phys.* **71** 1
[2] Ticknor C 2008 *Phys. Rev. Lett.* **100** 133202
Ticknor C 2007 *Phys. Rev.* A **76** 052703
[3] Ticknor C and Bohn J L 2005 *Phys. Rev.* A **72** 032717
[4] Bohn J L and Ticknor C 2005 *Proc. XVII Int. Conf. on Laser Phys.* ed E Hinds, E Ferguson and E Riis p 207
[5] Roudnev V and Cavagnero M 2009 *Phys. Rev.* A **79** 014701
[6] Roudnev V and Cavagnero M 2009 *J. Phys. B: At. Mol. Opt. Phys.* **42** 044017
[7] Cavagnero M and Newell C 2009 *New J. Phys.* **11** 055040
[8] Brink D M and Satchler G R 1993 *Angular Momentum* (Oxford: Clarendon)
[9] Werner J, Griesmaier A, Hensler S, Stuhler J, Pfau T, Simoni A and Tiesinga E 2005 *Phys. Rev. Lett.* **94** 183201
[10] Pavlović Z, Krems R V, Côté R and Sadeghpour H R 2005 *Phys. Rev.* A **71** 061402
[11] Shakeshaft R 1972 *J. Phys. B: At. Mol. Phys.* **5** L115
[12] Gao B 2008 *Phys. Rev.* A **59** 2778
Gao B 2008 *Phys. Rev.* A **78** 012702
[13] Stuhler J *et al* 2007 *J. Mod. Opt.* **54** 647
[14] Marinescu M and You L 1998 *Phys. Rev. Lett.* **81** 4596
[15] Deb B and You L 2001 *Phys. Rev.* A **64** 022717
[16] Ronen S, Bortolotti D C E, Blume D and Bohn J L 2006 *Phys. Rev.* A **74** 033611
[17] Derevianko A 2003 *Phys. Rev.* A **67** 033607
Derevianko A 2005 *Phys. Rev.* A **72** 039901 (erratum)
[18] Wang D-W 2008 *New. J. Phys.* **10** 053005

[19] Kanjilal K, Bohn J L and Blume D 2007 *Phys. Rev.* A **75** 052705
[20] Buchler H P *et al* 2007 *Phys. Rev. Lett.* **98** 060404
[21] Baranov M A 2008 *Phys. Rep.* **464** 71
[22] Mott N F and Massey H S 1965 *The Theory of Atomic Collisions* 3rd edn (Oxford: Clarendon) chapter XIV
[23] Bohn J L 2000 *Phys. Rev.* A **62** 032701
[24] Sawyer B C, Lev B L, Hudson E R, Stuhl B K, Lara M, Bohn J L and Ye J 2007 *Phys. Rev. Lett.* **98** 253002
[25] Sadeghpour H R, Bohn J L, Cavagnero M J, Esry B D, Fabrikant I I, Macek J H and Raub A R P 2000 *J. Phys. B: At. Mol. Opt. Phys.* **33** R93
[26] Johnson B R 1973 *J. Comput. Phys.* **13** 445
[27] Yi S and You L 2001 *Phys. Rev.* A **63** 053607
[28] Avdeenkov A V and Bohn J L 2005 *Phys. Rev.* A **71** 022706
[29] Bransden B H and Joachain C J 1983 *Physics of Atoms and Molecules* (Reading, MA: Addison-Wesley)
[30] Glauber R J 1959 *Lectures in Theoretical Physics* vol 1 ed W E Brittin *et al* (New York: Interscience)
[31] Navelet H and Wallon S 1998 *Nucl. Phys.* B **522** 237
[32] Gallagher T F 1994 *Rydberg Atoms* (New York: Cambridge University Press) p 293
[33] DeMille D, Glenn D R and Petricka J 2004 *Eur. Phys. J.* D **31** 375
[34] Kajita M 2002 *Eur. Phys. J.* D **20** 55
Kajita M 2004 *Eur. Phys. J.* D **31** 39
[35] Bohn J L, Burke J P Jr, Greene C H, Wang H, Gould P L and Stwalley W C 1999 *Phys. Rev.* A **59** 3660
[36] Ni K-K *et al* 2008 *Science* **322** 231
[37] Avdeenkov A V and Bohn J L 2002 *Phys. Rev.* A **66** 052718